

MOTORCYCLE IMPACTS INTO ROADSIDE BARRIERS – REAL-WORLD ACCIDENT STUDIES, CRASH TESTS AND SIMULATIONS CARRIED OUT IN GERMANY AND AUSTRALIA

F. Alexander Berg

Peter Rücker

Marcus Gärtner

Jens König

DEKRA Automobil GmbH

Germany

Raphael Grzebieta

Roger Zou

Monash University

Australia

Paper Number 05-0095

ABSTRACT

Roadside protection systems such as steel guard rails or concrete barriers were originally developed to protect occupants of cars and/or trucks – but not to protect impacting motorcycle riders. Motorcycle rider crashes into such barriers have been identified as resulting in severe injuries and hence has become a subject of road safety research. The German Federal Highway Research Institute (BASt) requested DEKRA Accident Research to analyse real-world crashes involving motorcycles impacting road side barriers and to identify typical crash characteristics for full-scale crash tests of a conventional steel system and a concrete barrier. A study of 57 real-world crashes identified two crash test scenarios which have been carried out: one with the motorcycle driven in an upright position and one with the motorcycle with the rider sliding on the road surface. The pre-crash velocity chosen was 60 km/h. The impact angle was 12° for the upright driven motorcycle and 25° for the motorcycle and rider sliding.

Two crash tests have been conducted to analyse impacts onto conventional steel guard rails and two tests to analyse impacts onto a concrete barrier. Two additional full-scale crash tests were carried out to analyse the behaviour of a modified roadside protection system made from steel.

A second phase of the work involved carrying out computer simulations at Monash University's Department of Civil Engineering. The DEKRA results from the crash test, where the upright motorcycle impacts the concrete barrier, were used to validate a MADYMO motorcycle-barrier model. This model was then used to investigate other impact speeds, a 25° impact angle scenario and different impact scenarios between an upright motorcycle and a wire rope barrier system. The results revealed; that the risk for motorcyclists of

being injured when colliding with either a wire rope or a concrete barrier will be high.

The paper describes the relevant real-world accident scenarios, the different roadside protection systems used for the tests, the crash tests, the modelling simulations and the results, and proposes improvements to barrier systems to reduce injury severity.

INTRODUCTION

In Germany, the most common roadside protection systems are guard rails made from steel. Concrete barriers are also in use. All the systems are described in a technical regulation [1]. The systems have to meet test criteria described in DIN EN 1317 [2]. The protection systems and the corresponding regulations were originally developed to protect occupants of cars and/or trucks – but not to protect impacting motorcyclists.

A similar situation exists in Australia. AS3845 [3], AS 1742.3 [4] and AS 5100.2 [5] are the standards that specify how permanent and/or temporary barriers are to be designed, used or tested for roadside and bridge barrier systems. Each State regulatory authority also has its own road design guidelines that further complicate barrier specifications. Whilst AS3845 discusses and considers impacts by motorcyclists, there are no references to any barrier systems specifically designed for protecting motorcyclists.

Some motorcycle rider crashes into steel guard rails, wire rope and concrete barriers have been identified as resulting in severe injuries and hence has become a subject of road safety research.

The German Federal Highway Research Institute (BASt) requested DEKRA Accident Research to analyse real-world crashes involving motorcycles impacting road side barriers and identify typical crash characteristics for further full-scale crash tests

using the mostly involved conventional steel-made systems and a concrete barrier (see Figure 1.).

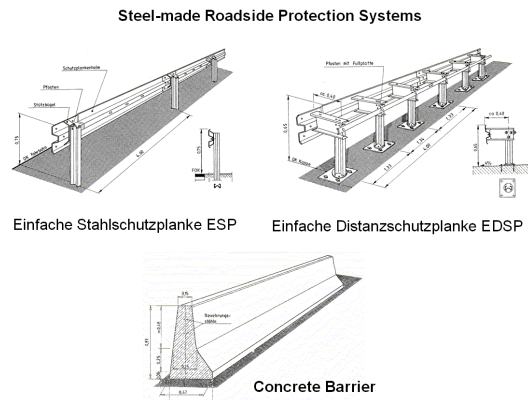


Figure 1. Two steel-guard rails and a concrete barrier common for German roads and investigated with full-scale crash tests

REAL-WORLD CRASHES

There are no federal statistics available for Germany identifying accidents related to motorcyclists impacting a roadside protection system. Forke [6] analysed detailed accident data from France and Austria. He predicted that 4.7% of all crashes involving injured motorcycle riders is related to impacts onto a roadside protection system. This indicates around 1,808 crashes occur where motorcycle riders are injured, can be estimated for Germany in the year 2003 (4.7% of all 38,464 crashes involving injured motorcycle riders registered for this year).

To calculate the total number of accidents where motorcycle riders are killed, Forke uses again French and Austrian accident data and also German data collected from a region around the city of Tübingen. He calculated such crashes to contribute 9.75 to 15% of all fatal crashes. This is around 92 to 114 accidents where motorcyclists are killed for the year 2003 in Germany that are related to impacts onto roadside protection systems (9.75 to 15% of all 38,464 crashes with injured motorcyclists for this year).

The DEKRA Accident Research Unit analysed 57 real-world crashes involving impacts of motorcycle, and respectively the rider, onto a roadside protection system.

An example of a real-world crash is given in Figure 2. The motorcycle was driven around a left-hand bend. Its speed was reconstructed to be in the range of 85 – 95 km/h. The driver lost control and the motorcycle tilted onto its side. This was followed by an impact of the motorcycle with the rider sliding on the road surface onto the roadside protection system. The protection system is a so called “einfache Schutzplanke” ESP (see Figure

1.). The profile of its posts is similar to the Greek letter Σ (Sigma). Therefore the post is called a “Sigma Post”. The rider’s neck directly impacted the post. It is reported that he suffered severe injuries (AIS 5) such that his neck was broken directly underneath neck vertebra C1. He also suffered internal injuries from additional impacts. The motorcyclist died after the accident.

63% of the 57 cases analysed by DEKRA involved a steel barrier “Einfache Stahlschutzplanke” ESP (Figure 1.). The second most frequently struck barrier, comprising 18% of all such crashes was another steel-made system, the so called “Einfache Distanzschutzplanke” EDSP (Figure 1.).

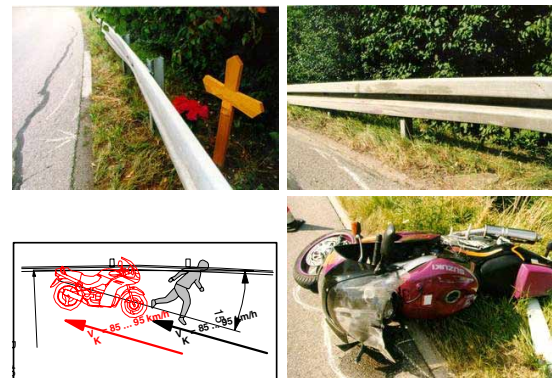


Figure 2. Example of a real-world crash

The DEKRA study also showed that in 51 % of the 57 cases analysed the motorcycle impacted the barrier while driving in an upright position whereas 45% of the impacts occurred where the motorcycle slid on its side on the road surface before it first struck the barrier. In 4% of the crashes the motorcycle impacted the barrier driving in an inclined position (not completely over on its side). In regards to road geometry, 53% being the majority of the crashes occurred in left-hand bends, 50% occurred on straight roads and 7% in right-hand bends.

CRASH TESTS AND RESULTS

Two impact scenarios were chosen for the full-scale crash test program as a result of the findings from the real-world crash study. In the first impact scenario the motorcycle was driven in an upright position (Figure 3) prior to impact. In the other scenario the motorcycle struck the barrier while skidding on its side (Figure 4).

For all crash tests the pre-crash velocity of the motorcycle was 60 km/h. For the impacts where the motorcycle was driven upright the angle between its velocity vector and the barrier was 12°. For the impacts where the motorcycle skidded on the ground the angle between its velocity vector and the barrier was 25°.

All tests were carried out with the same make, model and type of motorcycle being a Kawasaki ER 5 Twister (Figure 5.). The mass of the motorcycle itself was approx. 180 kg and approx. 272 kg with the dummy sitting on the motorcycle and wearing standard protective clothing.

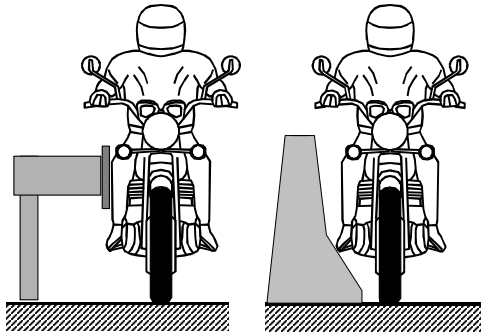


Figure 3. Test where the motorcycle impacted the barrier in an upright driving position

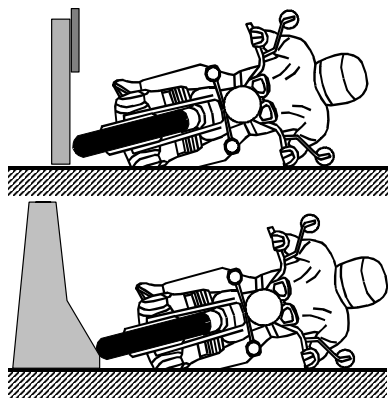


Figure 4. Test where the motorcycle impacted the barrier skidding on its side



Figure 5. Motorcycle Kawasaki ER 5 Twister as used for all crash tests

The Motorcycle rider was represented by a Hybrid III dummy (50th percentile male, hip the

same as for a “standing ATD”). To evaluate the injury risk of the rider, the rider’s initial contact “primary” impact into the roadside protection system, the “secondary” impact onto the ground and the movement alongside the roadside protection system were assessed using measured dummy loads and by analysing high speed films.

Impacts with the motorcycle moving in upward driving condition

Steel Guard Rail

Figure 6 shows the test with the motorcycle leaving the sled at 60 km/h and impacting at 58 km/h in an upright position the so called “Einfache Distanzschutzplanke” EDSP.

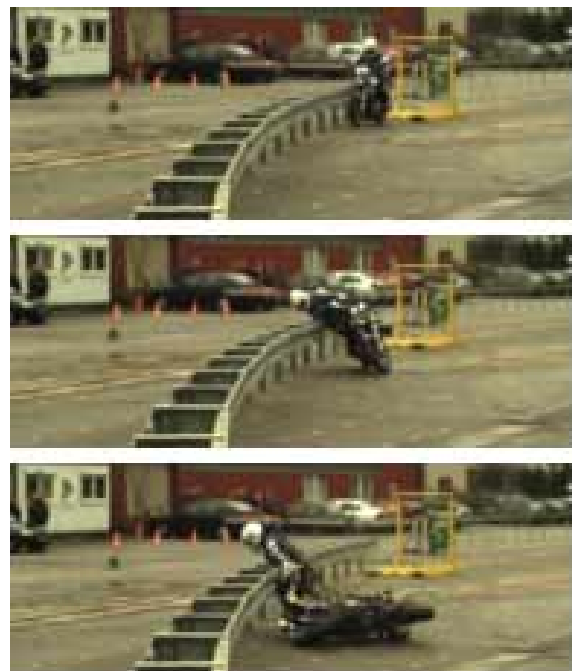


Figure 6. Full-scale crash test where the motorcycle impacted the steel guard rail “Einfache Distanzschutzplanke” EDSP in an upright position

During this test the dummy slides alongside and onto the steel guard rail. Here, the rider would have suffered severe injuries especially to the shoulder, the chest and the pelvis corresponding to aggressive contacts and snagging with some of the roadside protection system’s stiff parts and open profiles.

Figure 7 further illustrates the movement trajectories of the motorcycle and the rider determined from analysis from the films of the overhead-view cameras for a time period of 300 milliseconds after impact into the guard rail. The motorcycle reaches its final rest position 28 m after the point of first contact with the barrier. The distance between the point of first contact and the final rest position of the dummy was 21 m.

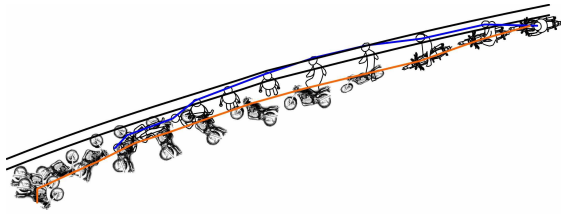


Figure 7. Trajectory of the motorcycle and rider during the first 300 milliseconds after impacting the steel guard rail system EDSP (see Figure 6) determined from analysis of the overhead-view cameras

Measured dummy loads for the head, the chest, the pelvis and the femur corresponding to the moment of first “primary” impact into the guard rail and the “secondary” impact onto the road surface are shown in Table 1. These measurements do not indicate a high-level injury risk. The compressive force of the right femur during the primary impact of 2.6 kN is somewhat high but clearly beneath the limit of 10 kN.

Table 1. Measured dummy loads for the full-scale crash test shown in Figure 6

| Dummy load | Primary impact | Secondary impact | Biomechanical limit |
|-------------------|----------------|------------------|---------------------|
| Head HIC | 4 | 277 | 1,000 |
| Head a_{3ms} | 9 g | 74 g | 80 g |
| Chest a_{3ms} | 13 g | n. a. | 60 g |
| Pelvis a_{3ms} | 7 g | 10 g | 60 g |
| Femur F_{left} | 0 kN | 4.1 kN | 10 kN |
| Femur F_{right} | 2.6 kN | 0.2 kN | 10 kN |

Concrete barrier

The concrete barrier (Figure 8) does not have any aggressive open shaped parts as in the case of the steel-based systems. In this crash test the motorcycle left the sled at 60 km/h prior to impacting the barrier. This was followed by the dummy flying over the top of the barrier. The dummy reached its final rest position on the opposite side of the barrier (Figure 8 and Figure 9). The distance of the final rest position from the point of first contact primary impact location was 26 m for the dummy and 38 m for the motorcycle.



Figure 8. Full-scale crash test of a motorcycle impacting a concrete barrier protection system in an upright position prior to impact moving

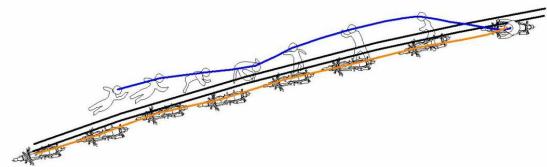


Figure 9. Motorcycle and rider trajectories during the first 175 milliseconds after impacting the concrete barrier (Figure 8) as determined from analysis of the overhead-view cameras

Table 2. Measured dummy loads for the full-scale test shown in Figure 8

| Dummy load | Primary impact | Secondary impact | Biomechanical limit |
|-------------------|----------------|------------------|---------------------|
| Head HIC | 0 | 164 | 1,000 |
| Head a_{3ms} | 3 g | 47 g | 80 g |
| Chest a_{3ms} | 4 g | 20 g | 60 g |
| Pelvis a_{3ms} | 11 g | 29 g | 60 g |
| Femur F_{left} | 0 kN | 0.6 kN | 10 kN |
| Femur F_{right} | 4.5 kN | 0.1 kN | 10 kN |

The measured dummy loads again do not indicate any life-threatening injury risk (see Table 2.). The right femur is subjected to a compressive load of 4.5 kN being clearly below the injury limit of 10 kN.

Analysis of the film revealed that the motorcycle and the rider were effectively not decelerated during contact with the concrete barrier. As a consequence of this the risk of being deflected by the barrier into oncoming-traffic on the road is clearly higher than for a barrier protection system made from steel. Another disadvantage of concrete barriers is that during an impact they do not dissipate as much kinetic energy via deformation as the systems made from steel.

Impacts where the motorcycle slides on its side

Steel Guard Rail

Figure 10 shows the test where the motorcycle slides-on its side and impacting the so called “einfache Schutzplanke” ESP (Figure 1).



Figure 10. Full-scale crash test where-the motorcycle impacts the protection system “Einfache Stahlschutzplanke” ESP by sliding into the barrier

The motorcycle’s velocity leaving the sled was 60 km/h. It directly impacted a sigma post at 47 km/h that broke and was bent down to the ground. Immediately after this first primary impact the motorcycle was stopped and remained stuck underneath the guard rail. The dummy separated from the motorcycle and collided with a sigma post. The distance between the location of the primary impact point and the final rest position was 2 m for the motorcycle and 5 m for the dummy.

Figure 11 shows the trajectories of the motorcycle and dummy before and after impact onto the

protection system as determined from the analysis of the film from the overhead-view cameras.

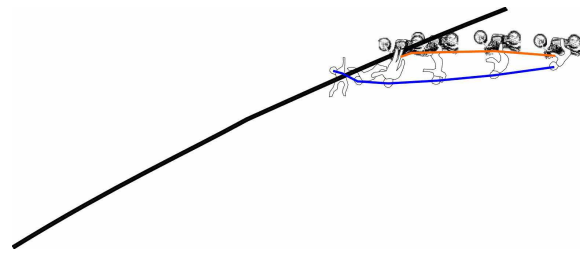


Figure 11. Trajectories determined from the overhead-view cameras of the motorcycle and the dummy before and after impacting the steel guard rail (Figure 10)

Table 3 gives an overview of some of the dummy loads measured at the point of first impact onto the protection system and from the second impact onto the ground. Very high loads above the biomechanical limits were measured for the head during the first contact primary impact. Due to the hard impact into the post, the left shoulder joint of the dummy was broken.

Table 3. Measured dummy loads for the full-scale test shown in Figure 10

| Dummy load | Primary impact | Secondary impact | Biomechanical limit |
|-------------------|----------------|------------------|---------------------|
| Head HIC | 1,074 | 66 | 1,000 |
| Head a_{3ms} | 125 g | 28 g | 80 g |
| Chest a_{3ms} | 39 g | 39 g | 60 g |
| Pelvis a_{3ms} | 15 g | 57 g | 60 g |
| Femur F_{left} | 3.4 kN | 1.2 kN | 10 kN |
| Femur F_{right} | 0.5 kN | 2.4 kN | 10 kN |

Concrete barrier

The impact where the motorcycle slides onto its side into the concrete barrier is shown in Figure 12. The motorcycle left the sled at 59 km/h and the front wheel impacted the barrier at 46 km/h.

The trajectories resulting from the analysis of the films from the overhead-view cameras are shown in Figure 13.

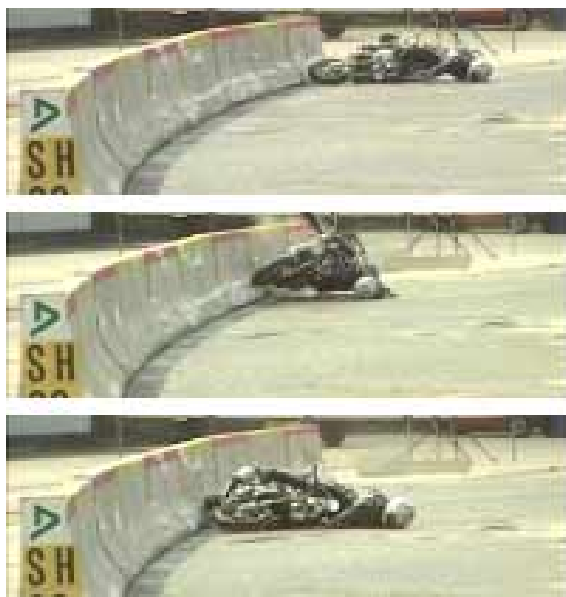


Figure 12. Full-scale crash test where the motorcycle impacts the concrete barrier protection system in a sliding position

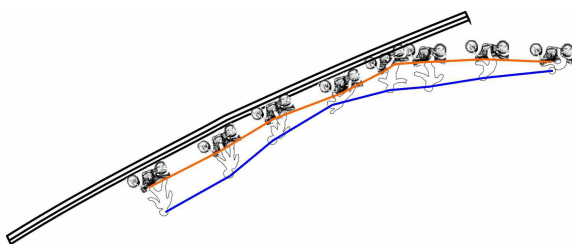


Figure 13. Overhead-view film analysis of test shown in Figure 12 showing the movement of the motorcycle and the dummy before and after impacting the concrete barrier protection system

Table 4. Measured dummy loads for the full-scale test shown in Figure 12.

| Dummy load | Primary impact | Secondary impact | Biomechanical limit |
|-------------------|----------------|------------------|---------------------|
| Head HIC | 1,346 | 1 | 1,000 |
| Head a_{3ms} | 135 g | 8 g | 80 g |
| Chest a_{3ms} | 50 g | 4 g | 60 g |
| Pelvis a_{3ms} | 16 g | 4 g | 60 g |
| Femur F_{left} | 4.1 kN | 3.0 kN | 10 kN |
| Femur F_{right} | 1.6 kN | 0 kN | 10 kN |

Some of the measured dummy loads related to the point of first impact into the protection system and to the second impact onto the ground are shown in table 4.

Deceleration of the motorcycle and dummy were not as rapid as during the impact where the motorcycle slid into the guard rail made from steel. Nevertheless the measured dummy decelerations for the primary impact were high, indicating a risks of severe and life-threatening injuries. The dummy head loads again lay clearly above the corresponding biomechanical limits.

Impacts into a modified steel guard rail system

The analysis of real-world crashes and the results of the crash tests shown above provided the technical basis to improve conventional roadside barriers made from steel with respect to protecting motorcyclists. As a first attempt a modified protection system was proposed and tested.

Figure 14 provides some information in regards to structure and the geometry of the modified system. The system is a so called “Schweizer Kastenprofil” consisting of sigma posts and a closed box-shaped profile at the top. An additional underrun protection board was mounted near to the ground to prevent both the direct impact onto a post and movement of the motorcyclist underneath the barrier protection system.

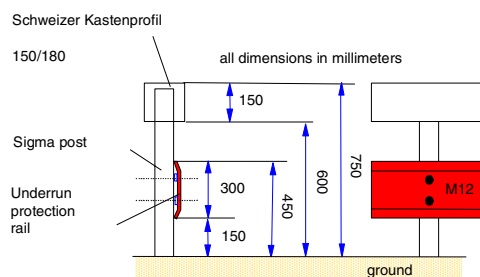


Figure 14. Modified guard rail system with respect to better protection for impacting motorcyclists

Two additional full-scale crash tests were carried out to analyse the behaviour of this modified roadside protection system where the rider was in the upright-impact position and a scenario where the impacting motorcycle and rider were sliding on the road surface.

Impact where the motorcycle is in an upright position

Figure 15 shows the crash test where the motorcycle and dummy is moving upright at 60 km/h and impacting the modified steel guard rail barrier system at 12°. After first contact into the barrier the motorcycle was redirected away from the barrier. The dummy separated from the motorcycle and fell onto the protection system. After sliding for a short distance on the guard rail the dummy fell to the ground on the opposite side. Because of the closed shape of the box-type profile, snagging did not occur and injury risk from impact was low as observed from the analysis of the film.

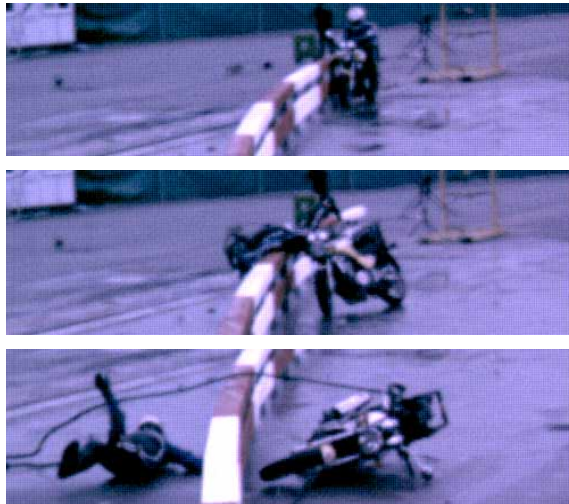


Figure 15. Full-scale crash test where the motorcycle impacts the modified steel guard rail system in an upright position

The trajectories of the motorcycle and dummy before and after impact onto the protection system determined from the analysis of the film from the overhead-view cameras is shown in Figure 16. The characteristics of the trajectories are similar to the corresponding crash test onto the concrete barrier (compare Figure 8 and Figure 9 to Figure 15 and Figure 16). The motorcycle reached the final rest position 23 m after initial contact primary impact. In the case of the dummy, the distance between the location of the initial primary impact and the final rest position was measured as 22 m.

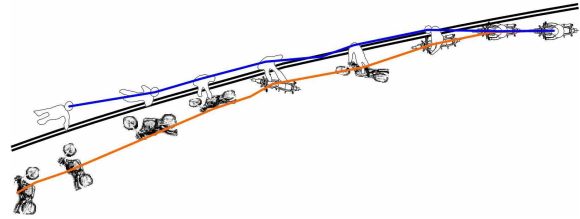


Figure 16. Trajectories of the motorcycle and dummy determined from the overhead view camera before and 230 milliseconds after impacting the modified steel guard rail system (see Figure 15)

Measured dummy loads related to the initial primary impact into the protection system and to the secondary impact onto the ground are shown in Table 5. Except for the left and right femur all measured loads of the other body parts are low and clearly beneath the corresponding biomechanical limits.

A compressive force of 6.3 kN for the right femur during the primary impact, 9.3 kN for the left femur and 6.5 kN for the right femur during the secondary impact, were markedly higher - compared to the corresponding results of the tests involving the concrete barrier and the unmodified steel guard. Even though this result was disappointing it could also be interpreted as an example of a worst-case condition. For instance, it was observed from the film sequences that the secondary impact of the dummy onto the ground occurred such that both legs initially struck the ground at the same time resulting in relatively high deceleration of the torso.

Table 5. Measured dummy loads for the full-scale test shown in Figure 15.

| Dummy load | Primary impact | Secondary impact | Biomechanical limit |
|-------------------|----------------|------------------|---------------------|
| Head HIC | 1 | 103 | 1,000 |
| Head a_{3ms} | 3 g | 36 g | 80 g |
| Chest a_{3ms} | 3 g | 17 g | 60 g |
| Pelvis a_{3ms} | 9 g | 11 g | 60 g |
| Femur F_{left} | 0 kN | 9.3 kN | 10 kN |
| Femur F_{right} | 6.0 kN | 6.5 kN | 10 kN |

Impact where the motorcycle slides into the barrier

Figure 17 shows the crash test where the motorcycle and dummy slides on the road surface. The motorcycle left the sled at 60 km/h and impacted the barrier at 54 km/h. Due to the impact the underrun protection board broke and the motorcycle struck a Sigma post. The dummy separated from the motorcycle immediately after the initial primary impact and then the helmeted head struck the underrun protection board.



Figure 17. Full-scale crash test where the sliding motorcycle impacted the modified steel guard rail system

The trajectories of the motorcycle and dummy before and after the impact into the protection system determined from the analysis of the film from the overhead-view cameras is shown in Figure 18. The distance between the location of the initial primary impact and the final rest position is 1 m for the motorcycle and 7 m for the dummy.

Table 6 gives an overview of measured dummy loads related to the primary impact and to the secondary impact. For the primary impact into the protection system all measured dummy loads were clearly less than their corresponding injury tolerance limits. However the measured 3-ms-96 g head acceleration during the secondary impact is above the tolerance limit of 80 g. Also the HIC in the secondary impact with a value of 510 but clearly beneath the limit of 1,000 is relatively severe.

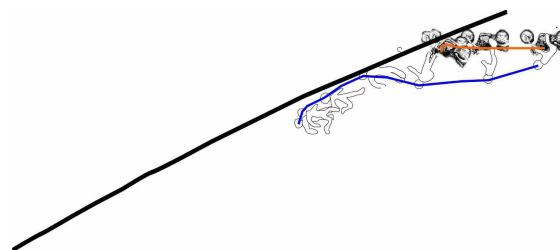


Figure 18. Trajectories of the sliding motorcycle and dummy determined from the overhead view camera before and after impacting into the modified steel guard rail system (see Figure 17)

Table 6. Measured dummy loads for the full-scale test shown in Figure 17

| Dummy load | Primary impact | Secondary impact | Biomechanical limit |
|-------------------|----------------|------------------|---------------------|
| Head HIC | 83 | 510 | 1,000 |
| Head a_{3ms} | 43 g | 96 g | 80 g |
| Chest a_{3ms} | 10 g | 31 g | 60 g |
| Pelvis a_{3ms} | 11 g | 19 g | 60 g |
| Femur F_{left} | 0.9 kN | 3.7 kN | 10 kN |
| Femur F_{right} | 3.6 kN | 0.4 kN | 10 kN |

In summary, the results from the crash tests show that the risk of injury for a motorcycle rider is much lower when impacting the modified system. The additional underrun protection board eliminated snagging of any parts of the impacting dummy. The additional board also absorbed kinetic energy as a result of its deforming during impact. However, the motorcycle was not redirected away from the protection system after initial impact. Hence, further improvements are still necessary to ensure the underrun protection board does not break and that the severity of the secondary impact onto the ground is reduced. Further questions arise whether the biofidelity of the Dummy Hybrid III is sufficient to accurately predict all injury risks a motorcyclist may be exposed to when impacting a roadside protection system and any subsequent impacts onto the road surface.

NUMERICAL SIMULATIONS

Monash University's Department of Civil Engineering has also carried out computer simulations to investigate motorcycle impacts into roadside barriers. The DEKRA results from the crash test, where the upright motorcycle impacts the concrete barrier, were used to validate a MADYMO motorcycle-barrier model. This model was then used to investigate other impact speeds, a 25° impact angle scenario and different impact scenarios between an upright motorcycle and a wire rope barrier system.

MADYMO Models

The MADYMO model consisted of four distinct systems; the road, the motorbike, the barrier and the rider. Two barrier types were modelled namely a concrete barrier and a wire rope barrier.

The road was assigned as the inertial space on which the motorbike, barrier and rider operated.

The motorcycle model with an adult male rider is shown in Figure 19. It represents a typical road motorbike with a dry weight of 240 kg.

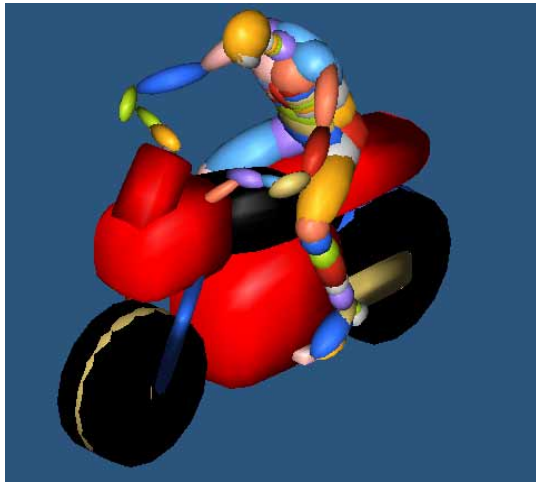


Figure 19 MADYMO motorcycle model

The stiffness properties for the wheels, engine, steel and fibreglass chassis used for the motorcycle model were selected based on previous experimentally validated crashworthiness studies of a variety of vehicles carried out by Zou and Grzebieta. Because the motorcycle was constructed as a multi-body system, parts of the motorbike surface area had to be constructed in such a way as to be able to interact with the concrete barrier, the wire rope barrier and the road surface.

The concrete barrier was modelled using a single ellipsoid with a height of 800 mm, a width of 200 mm and a length of 10 m. The barrier's weight was based on a material density of 2,500 kg/m³ and

hence was assigned a very high stiffness function so that there was minimal deflection of the barrier during the simulations.

The wire rope barrier model was based on an actual installed system (Figure 20 and Figure 21). This barrier consisted of seven posts that supported the four wires of the barrier. The wires of the barrier that were modelled are made up of three high tensile steel cables woven together with an assumed yield stress of 500 MPa. They have a combined circumference of 60 mm and were represented in the model by a TRUSS2 finite element with a cross sectional area of 280 mm² for each cable. The wires had an initial tension setting of 5 kN. Ellipsoids were used to model the support posts being 2 mm thick.

A non-helmeted 50th percentile adult male Hybrid III MADYMO model was used for the rider. The rider's seated position on the motorcycle is shown in Figure 19. The crash scenario where the rider was seated in an upright position was the only scenario analysed for the MADYMO model. Similarly only maximum value chest and head injuries were calculated and are listed here. No distinction was made between a primary or secondary impact.



Figure 20 Four rope wire rope barrier

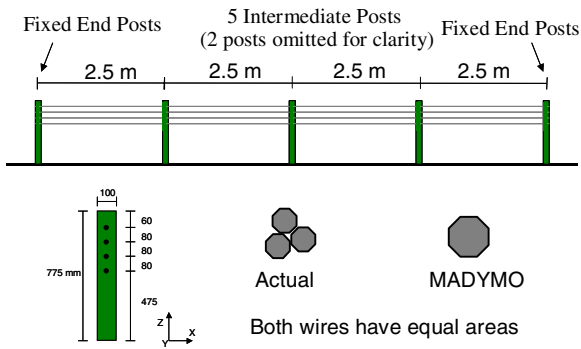


Figure 21 Wire rope barrier simulated in MADYMO

Simulation Results

Concrete barrier

Table 7 shows the resultant injury criteria from the DEKRA crash test compared to the MADYMO simulation where the rider impacts the concrete barrier in an upright position. Impact kinematics for an upright motorcycle with a rider impacting the concrete barrier are shown in Figure 22. The rider kinematics when compared to Figure 8 look similar. However the motorcycle seems to rebound from the wall, indicating further refinement of the model is required if it is to accurately model the actual crash test.

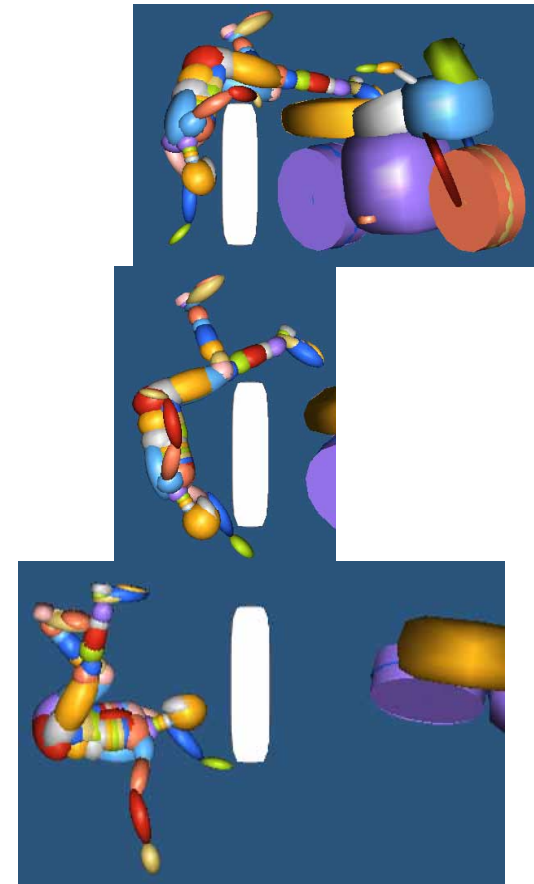
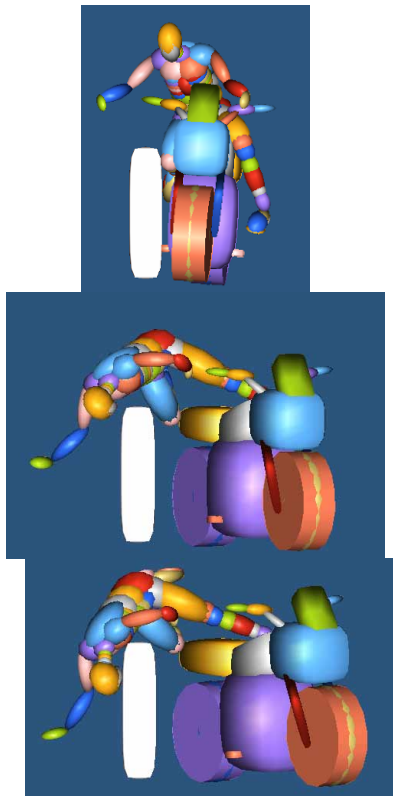


Figure 22 MADYMO simulation showing an upright seated rider on a motorcycle crashing into a concrete barrier at 60 kph and 12°

At a shallow impact angle (12°) the resulting calculated injury for the head and chest indicate that some form of injury is probable but is below threshold limits.

In each simulation the dynamics of the rider's fall to the ground were different. Consequently each simulation produces different injury values. For example in the 25° collision at 80 km/h the rider does a full vault landing feet first rather than head first. Hence a slightly lower HIC value is obtained when compared to the slower speed collision at the same angle.

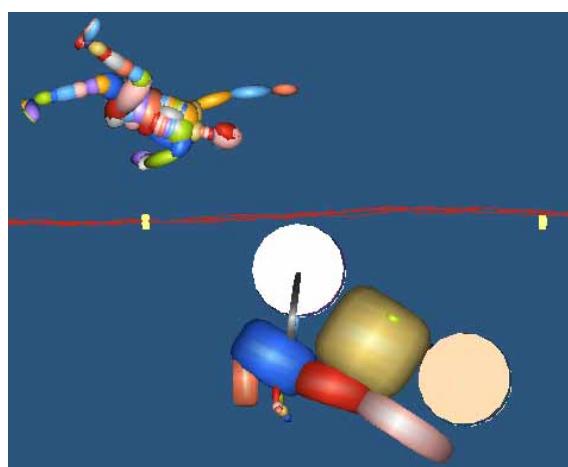
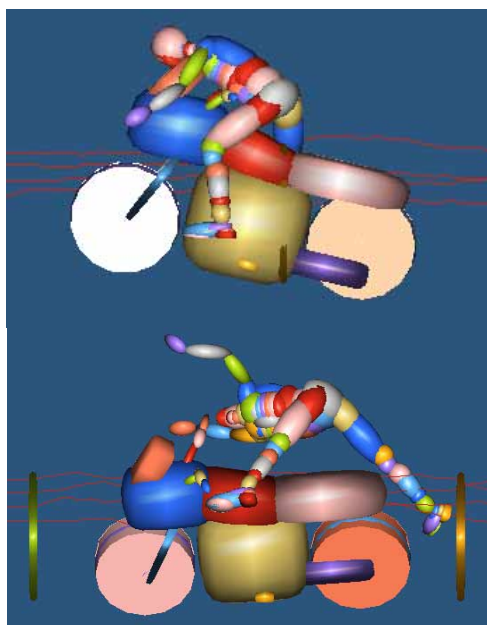
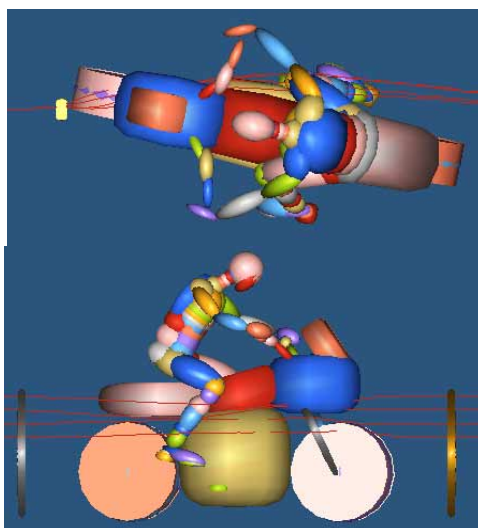


Figure 23 MADYMO simulation showing an upright seated rider on a motorcycle crashing into a wire rope barrier at 60 km/h and 12°

Table 7. Measured dummy loads for the full-scale test shown in Figure 17

| Simulation | Speed km/h | HIC 36ms | Chest g |
|--------------------------------|---------------|-------------|------------|
| DEKRA test | 60 | | |
| (primary impact) | | 0 | 4 |
| (secondary impact) | | 164 | 20 |
| 12° Concrete barrier | 60 | 44 | 15 |
| | 80 | 39 | 23 |
| 25° Concrete barrier | 60 | 133 | 32 |
| | 80 | 100 | 20 |
| 12° Wire rope | 60 | 462 | 68 |
| | 80 | 1205 | 100 |
| 25° Wire rope | 60 | 3,478 | 144 |
| | 80 | 4,879 | 41 |
| Injury criteria for a 50% male | | 1000 | 60g |

Wire rope barrier

Figure 23 shows the kinematics for an upright rider on a motorcycle impacting a wire rope barrier. The calculated injuries from the simulations suggest that serious injury would result regardless of speed and impact angle.

In all simulations the motorcycle slides along the wires until it hits a post, squeezing and trapping the rider's leg against the wires as it does so. The post contact causes the motorcycle's front wheel to snag lifting the front of the motorcycle up and throwing the rider's torso and head forward. Because the rider's leg is trapped between the motorcycle and the wire ropes and the foot snags in the ropes, the head and torso slap into the front of the rising motorcycle. Eventually the leg becomes free as the motorcycle rotates and the rider is then catapulted over the barrier. This is a different result to the concrete barrier where the rider was thrown over the barrier with relatively little snagging or deceleration.

In both the 60 km/h and 80 km/h impact speeds at an angle of 25°, the motorbike throws the rider into the air with the rider hitting the ground head first. Hence the high HIC.

One of the motorcycling community's key concerns with wire rope barriers was the possibility of a rider's limb(s) becoming caught in the barrier during a collision. The simulations seem to indicate that this snagging effect occurs for both the rider's leg nearest the barrier. However of greater concern is the snagging of the motorcycle's front wheel on the barrier's posts.

Discussion

Concerns have been raised by the motorcycling community about potential injuries resulting from collisions between motorcycles and wire rope barriers. To date little research has been undertaken to confirm or deny any concerns.

The concrete barrier simulations seem to indicate that a motorcyclist impacting such a barrier in an upright position will sustain survivable injuries because of low decelerations during impact. However, the motorcyclist is exposed to considerable risk when catapulted over the barrier into the hazard being protected by the barrier, particularly if it is a median barrier and there is oncoming traffic on the other side.

Simulations of the wire rope barrier collisions showed that regardless of angle or speed it is unlikely that the motorcyclist will clear the barrier very cleanly. In many cases the motorcyclist's extremities became caught between the wires. This results in the rider being subjected to high decelerations and possible high injury risk secondary impacts into the road.

In all the simulated wire rope barrier collisions, the wires guided the motorcycle into the posts leading to heavy contact with the post. The motorcycle and the rider were subjected to large decelerations because of this snagging effect and hence elevating the injury risk for the rider.

While the simulations in this report are preliminary, and work is continuing to refine the MADYMO models and calibrate them against the DEKRA tests, they show that the risk of injury to a motorcyclist colliding with either a wire rope or a concrete barrier will be high. The findings also suggest that while the current design of flexible barriers has safety advantages over concrete barriers for passenger vehicles, the opposite may be true for motorcyclists. Most of all, it has highlighted the need for further research into the area of motorcycle collisions with various crash barriers.

SUMMARY AND FUTURE WORK

Vehicle safety is still a major area of applied research, technical development and engineering. Large gains have been achieved in regard to the long-term reduction of road users killed and severely injured over two decades now. But further efforts are necessary to maintain the continual reduction of the "road toll" cost paid every year as a consequence of modern societies demand for mobility and transport on our roads.

From a political perspective example target objectives are outlined in the Commission of the European Community's White Paper "European

Transport Policy for 2010: Time to Decide" and in the "Vision Zero" legislation adopted by the Swedish Government. Common research objectives following an integrated holistic systems approach may provide the best potential to explore new options and/or better transform known solutions to improve vehicle and road safety in relation to the interaction between man, machine and infrastructure as a whole. The primary safety of vehicles has offered new perspectives but secondary safety seems to be offering further substantial gains in reducing road carnage.

In this context the safety of motorcyclists is also of interest. There are safety system options available and elements that can be fitted to motorcycles to improve their secondary safety. But the secondary safety of vehicles - and especially of motorcycles does not depend entirely on the crashworthiness performance of the vehicle itself.

Additional safety measures can be addressed by an actual research field called "compatibility". Compatibility currently only addresses the interaction of two vehicles crashing into each other and the balancing of self protection and partner protection seen as an integrated optimum. For secondary motorcycle safety the car's crashworthiness is very important as the most frequent crash partner in a motorcycle crash. However, the infrastructure, being compatible with cars, also needs to be considered in relation to motorcycle secondary "compatible" safety. As shown in the paper, research and engineering work dealing with motorcycle impacts onto roadside protection systems is another field of research where the secondary safety of motorcycle riders can be improved.

Last but not least there are some more options where motorcycle rider crashworthiness can be improved by further improving their clothing. Not only is the behaviour of helmets, jackets and trousers, under isolated test conditions to assess and improve the damping and/or abrasion resistance of interest, but there is also an integrated approach possible with additional improvements of the performance of safety elements and systems fitted to the motorcycle itself and to the motorcycle rider's clothing in relation to barrier impacts.

Not only should research continue into improving the crashworthiness of car and truck roadside barrier impacts but research into improving motorcycle rider impact crashworthiness should also be considered. The research program presented in this paper will continue both in regards to experimental testing either in Germany or Australia and in regards to computer simulations to improve models so that novel crashworthy designs to reduce motorcycle injuries can be investigated.

REFERENCES

- [1] Richtlinien für passive Schutzeinrichtungen an Straßen RPS. Forschungsgesellschaft für Straßen- und Verkehrswesen, Arbeitsgruppe für Verkehrsführung und Verkehrssicherheit, Ausgabe 1989
- [2] DIN EN 1317 Road restraint systems. DIN Deutsches Institut für Normung e.V.
- [3] Standards Australia, AS/NZS 3845 Australian / New Zealand Standard for Road Safety Barrier Systems, CE/33 Committee, ISBN 0 7337 2293 8, 1999.
- [4] Standards Australia, AS 1742.3: Manual of uniform traffic control devices Part 3: Traffic control devices for works on roads, Standards Australia, Sydney, ISBN 0 7337 4845 7, 2002.
- [5] Standards Australia, AS 5100.2: Bridge design Part 2: Design Loads, Standards Australia International, Sydney, ISBN 0 7337 5628 X, 2004.
- [6] Forke, E.: Das Schutzplankenprojekt aus Sicht der Motorradfahrer, Institut für Zweiradsicherheit (2002)
- [7] Bürkle, H. Berg, F. A.: Anprallversuche mit Motorrädern an passiven Schutzeinrichtungen. Berichte der Bundesanstalt für Straßenwesen, Reihe Verkehrstechnik, Heft V 90, Verlag für neue Wissenschaft GmbH, Bremerhaven, September 2001.